

Supporting Information

Strontium-calcium phosphate nanotubes as bioinspired building blocks for bone regeneration

*Camila B. Tovani¹, Tamires M. Oliveira¹, Mariana P. R. Soares², Nadine Nassif³,
Sandra Y. Fukada², Pietro Ciancaglini¹, Alexandre Gloter⁴, Ana P. Ramos^{1*}*

1. Departamento de Química, Faculdade de Filosofia, Ciências e Letras de Ribeirão Preto, Universidade de São Paulo, Ribeirão Preto, SP, Brazil

2. Departamento de Ciências Biomoleculares, Faculdade de Ciências Farmacêuticas de Ribeirão Preto, Universidade de São Paulo, Ribeirão Preto, SP, Brazil

3. Sorbonne Université, CNRS, Collège de France, Laboratoire de Chimie de la Matière Condensée de Paris, 4 Place Jussieu, F-75005 Paris, France

4. Laboratoire de Physique des Solides, Université Paris-Saclay, 91405 Orsay, France

*Corresponding author. E-mail : anapr@ffclrp.usp.br

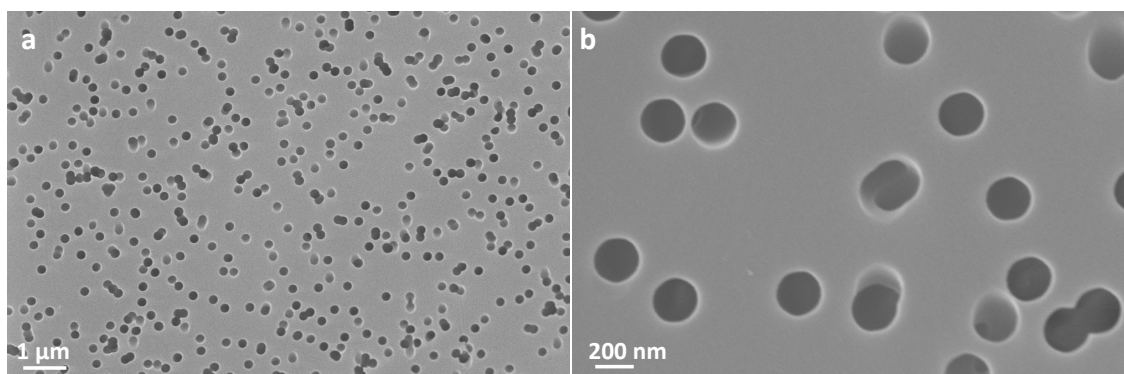


Figure S1. SEM images with different ampliation of the surface of a track-etched polycarbonate membrane showing homogeneously distributed cylindrical pores (a) with controlled morphology and size (b).

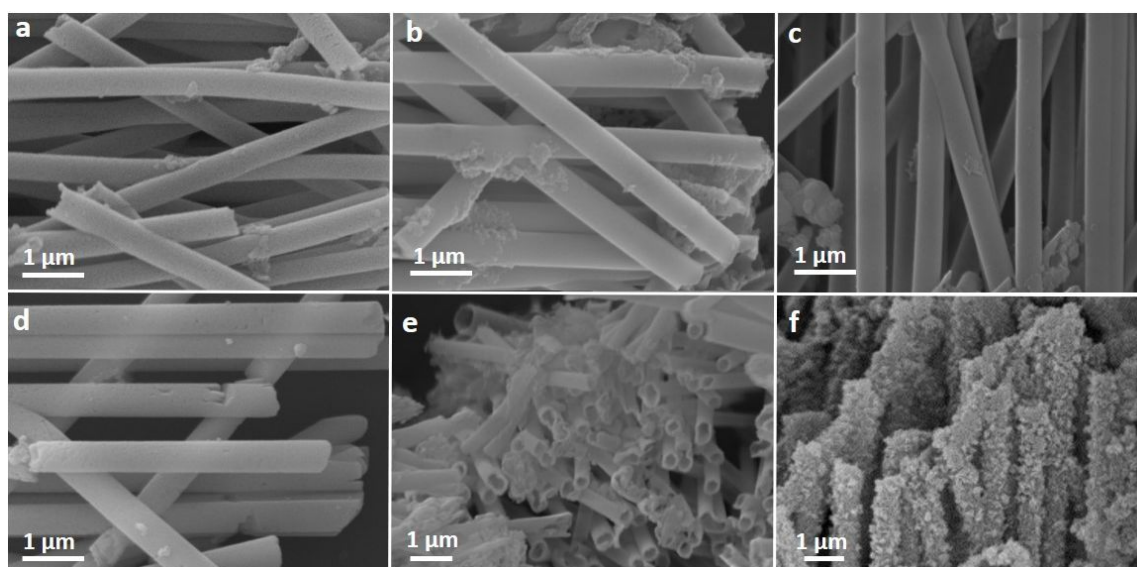


Figure S2. Submicrometer tubes formed in the track-etched membranes with 400 nm pores. SEM images of rod-like particles containing (a) 0% Sr^{2+} , (b) 10% Sr^{2+} , (c) 50% Sr^{2+} and (d) 100% Sr^{2+} . The particles are hole (e) and induce the precipitation of bone-like apatite after immersion in simulated body fluid for 5 days (f), as also observed for the 200 nm particles. Images (e) and (f) are representative from the 10% Sr^{2+} sample.

Table S1. Sr^{2+} molar percentages (% Sr^{2+}) in relation to the total number of mols of divalent cations ($\text{Ca}^{2+} + \text{Sr}^{2+}$) in the starting solutions and in the products formed in bulk and in confinement, determined by TEM-EDX

%Sr^{2+} in the solution	%Sr^{2+} bulk products	%Sr^{2+} confinement products
0	-	-
10	10	9
50	42	40
100	99	96

Table S2. Products formed in confinement and in bulk precipitations at different Sr^{2+} concentrations

%Sr^{2+}	Bulk products	Confinement products
0	Apatite+OCP	Apatite
10	Sr^{2+} substituted apatite	Sr(ACP)
50	Sr(ACP)	Sr(ACP)
100	SHP	Sr-apatite

* OCP = octacalcium phosphate, Sr(ACP) = strontium-loaded amorphous calcium phosphate
SHP = *strontium hydrogen phosphate*

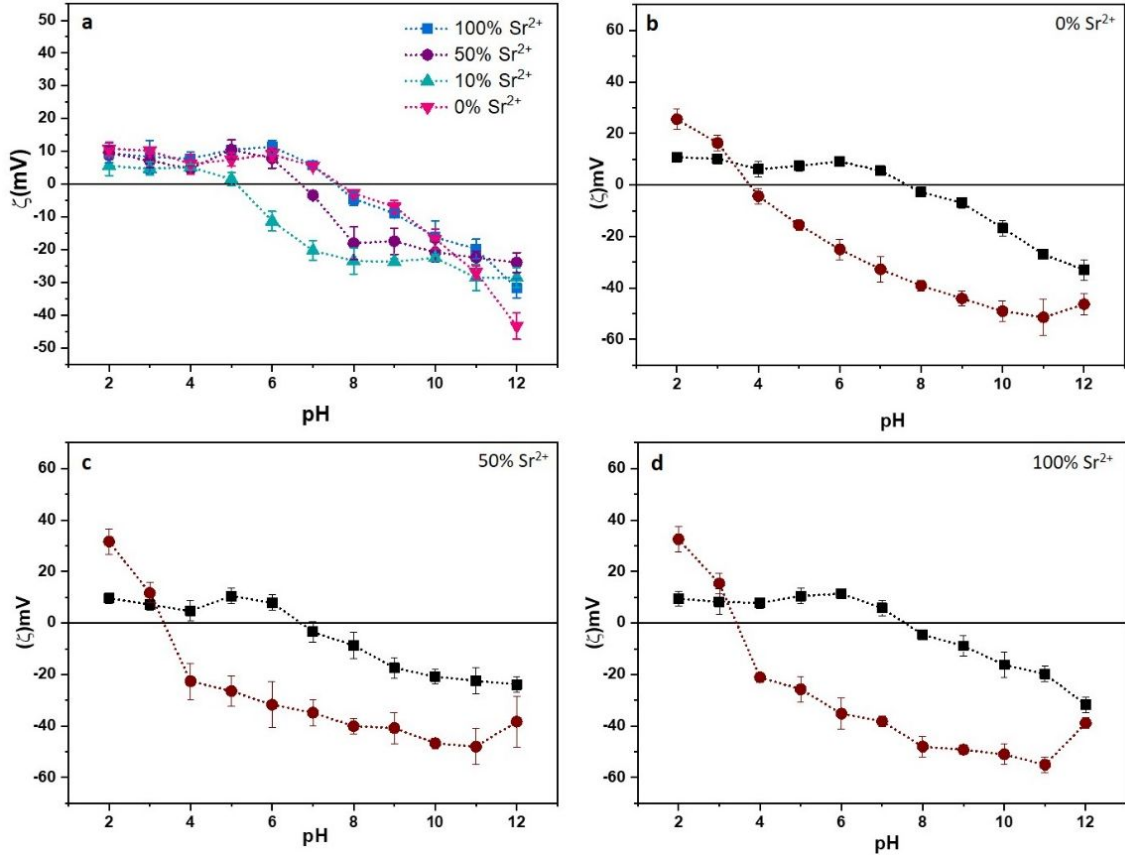


Figure S3. Zeta potential (ζ) versus pH curves obtained to the nanotubes containing different concentrations of Sr^{2+} . (a) The particles with amorphous structure (10% Sr^{2+} and 50% Sr^{2+}) display lower values of isoelectric point compared to the crystalline particles (0% Sr^{2+} and 100% Sr^{2+}). This may be ascribed to the different environments (crystalline *versus* amorphous) where the surface groups (OH , HPO_4^{2-}) are present. (b) The interaction of the particles with the constituents of the cell culture medium was evaluated by the ζ versus pH curves obtained before (black curve) and after (red curve) the immersion of the particles in the cell culture medium. The ζ were displaced towards negative values indicating the modification of the surface of the particles by the adsorption proteins.

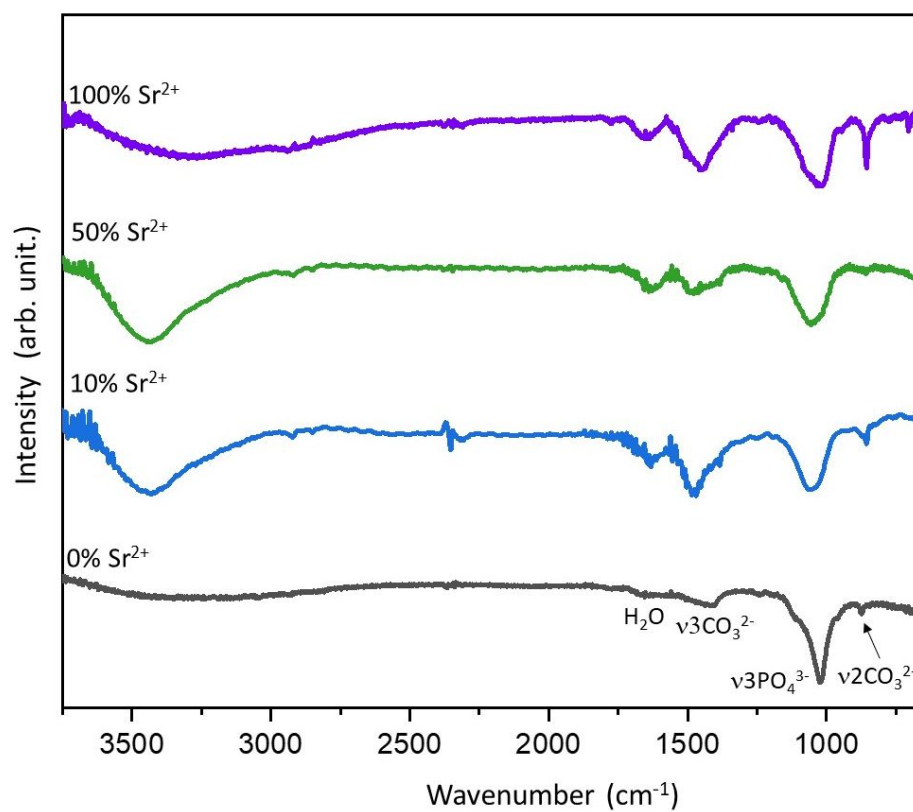


Figure S4. ATR-FTIR spectra of Sr(CaP) nanotubes. Bands ascribed to phosphate and carbonate groups and water molecules are observed.

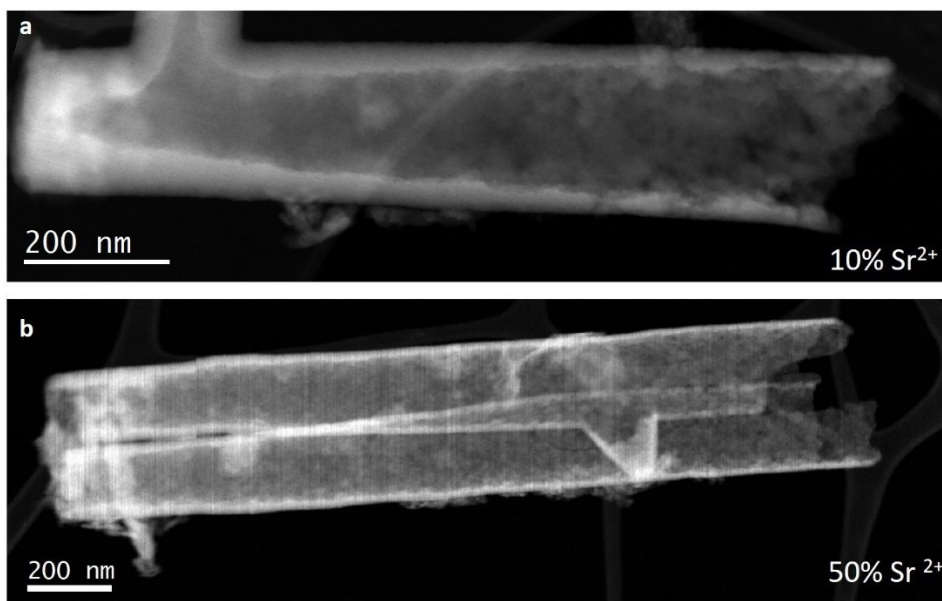


Figure S5. Low magnification STEM-HAADF images showing (a) “vase” shaped hollow rod (10% Sr²⁺) and (b) narrowing rod walls of a 50% Sr²⁺ nanotube.

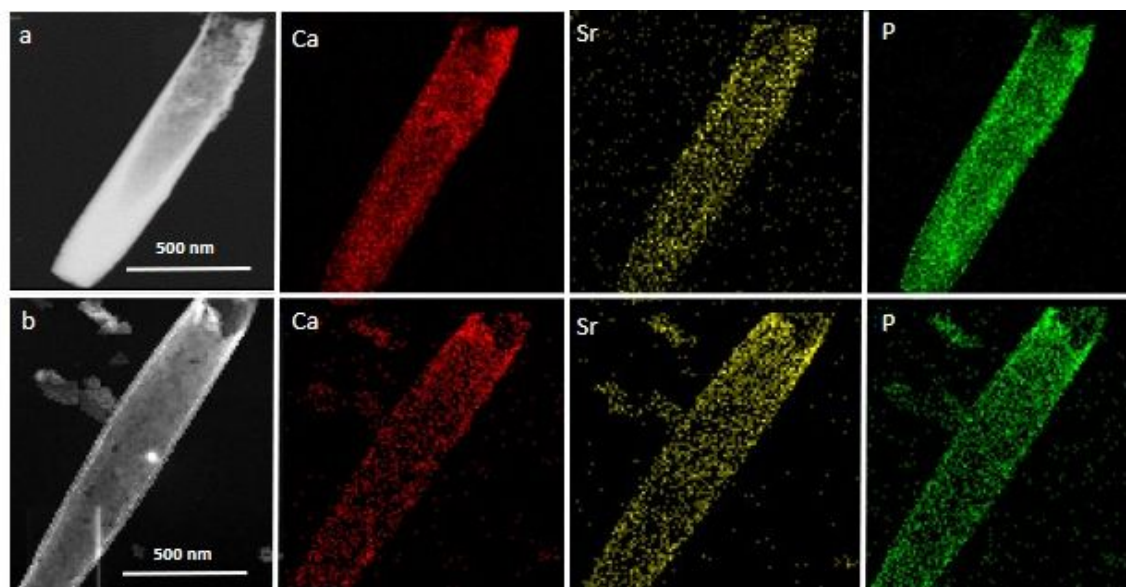


Figure S6. Dard field TEM images of the nanotubes containing (a) 10% Sr^{2+} and (b) 50% Sr^{2+} with TEM-EDX mapping profiles showing that Ca, Sr, and P are homogeneously distributed in the particles considering the EDX resolution.

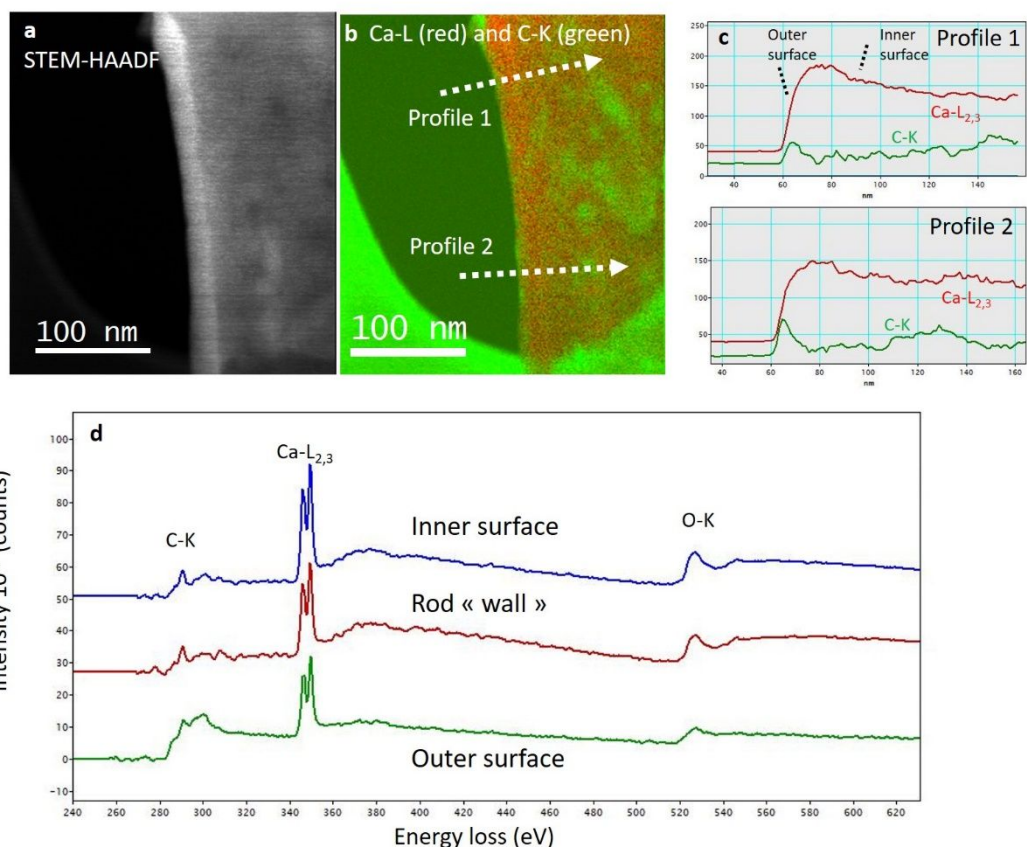


Figure S7. STEM-EELS measurement done with sample maintained at low temperature by LN₂ sample holder (STEM-VG microscope). a,b) HAADF images along with a C-K and Ca-L based chemical image of a 50% Sr tube. c) Profiles from the chemical image showing the presence of a nanometric layer of carbon at the outer surface of the rod. d) EELS spectra showing that the outer layer has a substantial contribution of an “amorphous carbon” type that might be the result of e-beam damage organic carbon. The rod “wall” and the inner surface mostly show the contribution from a carbonate type fine structure.

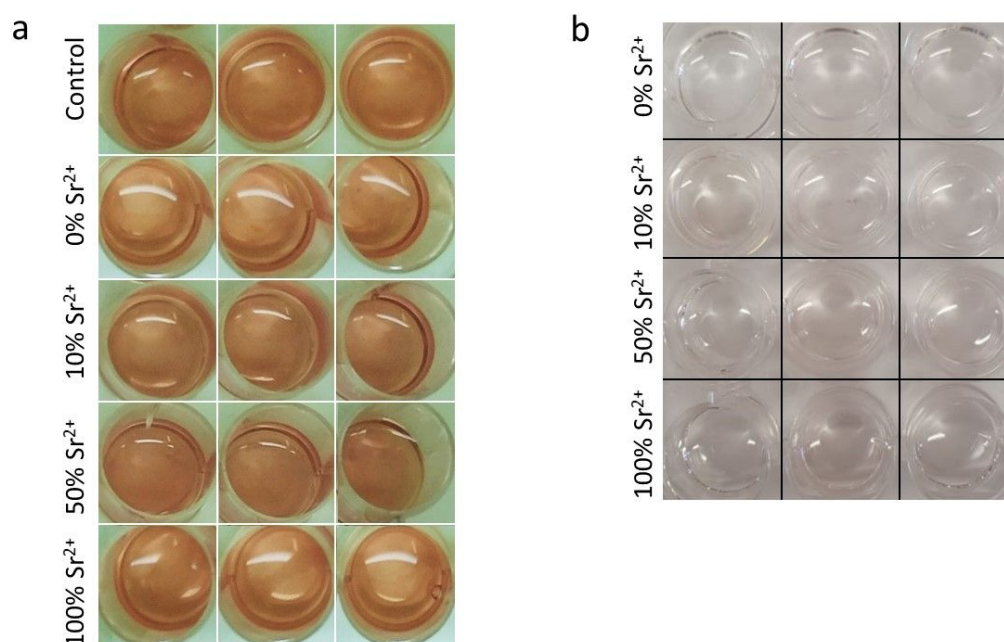


Figure S8. (a) Photographs of Alizarin Red S stained mineralization of osteoblasts cultured for 21 days in the absence (control) and in the presence of Sr(CaP) nanotubes. (b) Photographs of Alizarin Red S treated wells after exposure to a suspension of Sr(CaP) nanotubes and in absence of cells. As observed, the particles did not interfere with assay since the wells were washed with PBS removing possible precipitated particles from the culture medium. The colloidal stability of the particles also prevented their precipitation in the wells.